J. Appl. Comput. Mech., 6(3) (2020) 531-542
DOI: 10.22055/JACM.2019.29377.1593

ISSN: 2383-4536
jacm.scu.ac.ir

M&MoCS

Shahid Chamran University of Ahvaz

Journal of Applied and Computational Mechanics

Research Paper

Numerical Scrutinization of Three Dimensional Casson-Carreau Nano Fluid Flow

P. Naga Santoshi[1], **G.V. Ramana Reddy**[2], **P. Padma**[3]

[1] Research Scholar in Koneru Lakshmaiah Education Foundation
Vaddeswaram, Guntur, A.P, India, E-mail: pnagasantoshi@gmail.com

[2] Department of Mathematics, Koneru Lakshmaiah Education Foundation
Vaddeswaram, Guntur, A.P, India, E-mail: gvrr1976@gmail.com

[3] Department of Mathematics, Govt. Degree College, Yellandu, Bhadradri Kothagudem
Telangana, India, E-mail: padmapolarapu@gmail.com

Received May 04 2019; Revised September 19 2019; Accepted for publication September 21 2019.
Corresponding author: P. Naga Santoshi (pnagasantoshi@gmail.com)
© 2020 Published by Shahid Chamran University of Ahvaz
& International Research Center for Mathematics & Mechanics of Complex Systems (M&MoCS)

Abstract. This study presents the computational analysis of three dimensional Casson and Carreau nanofluid flow concerning the convective conditions. To do so, the flow equations are modified to nonlinear system of ODEs after using appropriate self-similarity functions. The solution for the modified system is evaluated by numerical techniques. The results show the impacts of involving variables on flow characteristics and the outcomes of the friction factors are evaluated as well. In this study, the outcomes to local Nusselt number and Sherwood numbers are evaluated. Favourable comparison is performed with previously available outcomes. The achieved results are similar to solutions obtained by other researchers. The results are presented for flow characteristics in the case of Casson and Carreau fluids. Velocities are reduced for the growing values of permeability and velocity slip parameters in case of Casson and Carreau nanofluids. Temperature field enhances with the hike in the estimations of thermophoresis parameter and the thermal Biot number in case of Casson and Carreau nanofluids. Enhancing values of velocity slip parameter results in decrease in the skin friction coefficients and the rate of heat transfer, and rise in the rate of mass transfer in case of Casson and Carreau nanofluids.

Keywords: Steady flow; Three dimensional flow; Casson Fluid; Carreau Fluid; Nano fluid; stretching Sheet; Convective condition.

1. Introduction

The inquiry of Non-Newtonian fluids is a significant subject matter and has dragged scientists' attention. The fluid has so many leading uses in engineering. It has used in technological procedures. These uses appear in chemical materials like drilling mud, pharmaceutical chemicals etc. Casson is the person who gave the non-Newtonian fluid version in 1995. Sakiadis [1] inquired the boundary layer flow behavior through a stretching surface. Chamka [2] studied the flow characteristics of a nanofluid through a vertical plate concerning the heat generation or absorption effects under different fascinating aspects. The article related to Nano fluid is found in reference [3]. Hasio [4] found that the energy conversion is utilization for thermal extrusion energy system. Nadeem et al. [5] predetermined the three dimensional scrutiny for the Casson fluid across the stretching sheet. Shehzad et al. [6] developed a numerical model for three dimensional flow of Casson fluid through a stretching surface. Raju et al. [7] reported the results that a hike in space and temperature dependent heat generation or absorption elevates the temperature field and concentration profile of the flow.

Published online: September 17 2019

Akbar et al. [8] have done their work upon the peristaltic flow of Carreau nanofluid. Akbar et al. [9] pursued their work upon stagnation point flow of MHD Carreau fluid.

The main intent of this work is to compute the dual solution for MHD Carreau fluid flow analysis upon a stretching sheet. Hayat et al. [10] confined their work with the convective boundary conditions in the mixed convention flow upon a stretching sheet. They formulated the problem in the existence of thermal radiation, heat source/sink and first order chemical reactions. The influence of certain important variables for velocity, energy and concentration profiles of Casson Carreau fluid flow are studied by Naga Santoshi et al. [11] through diagrams and tables. Hsiao [12] made examinations which are the numerical usage to a thermal extrusion producing technique frame work energy transformation issue by utilizing some improved variables control mechanism. Olanrewaju et al. [13] discussed flow characteristics of nanofluids concerning radiation. Hsiao [14] has obtained outcomes which exhibit that it generate more heat transfer impacts with bigger estimations of viscoelastic number, Prandtl number, free convection parameters, electric parameter (E1), heat source/sink (AL) and conduction-convection number (Ncc). The numerical results of Hsiao [15] show that an improving in the magnetic parameter decreases the estimation values of the velocities and Nusselt number, or a boosting in the estimates of the shear stress, couple stress at the surface, temperature and concentration. Sandeep et al. [16] have scrutinized the impact of different physical variables on fluid characteristics. Saleem et al. [18] have performed their work on the flow characteristics of slip flow. Sandeep and Sulochana [19] have computed the answers for fluid characteristics with the help of shooting mechanism. Raju et al. [20] investigated the influence of different variables upon the flow of Ferro-fluids with the existence of non-uniform heat source/sink and velocity slip. Bhatti and Lu [21] derived solution to head-on collision between two hydroelastic solitary waves in shallow water. As Lu et al. [22] analyzed the behavior of blood flow upon a capillary with gyrotactic microorganisms. Bhatti and Lu [23] obtained graphical comparative reports for special cases with pure-gravity waves. Bhatti and Rashidi [24] have combined the thermo-diffusion and thermal radiation impacts for describing Williamson nanofluid flow characteristics.

The intension of Naga Santoshi et al. [25] was to discuss the heat and mass transfer characteristics of mixed convective non-Newtonian nanofluid flow with non-uniform heat source/sink and variable viscosity. Hayat et al. [26] have examined the impacts of Cattaneo–Christov heat flux model. The study of flow characteristics upon a stretching sheet having homogeneous–heterogeneous reaction play significant role in metallurgy and chemical engineering industries, like polymer production and food processing. These problems have many industrial applications. Some articles related to homogeneous-heterogeneous reactions are given in references [27, 28, 29, 30]. Khan et al. [31] examined activation energy effect in nonlinear radiative stagnation point flow of cross nanofluid. The articles related to Entropy generation problem are shown in references [33-38]. Khan et al. [39] used RANS model for VIV study of mounted cylinder. Hayat et al. [40] studied the modern developments about statistical declaration and probable error for skin factor as well as Nusselt number with copper and silver nanoparticles. Raju et al. [41] investigated the flow characteristics in MHD Casson fluid. Hayat et al. [42] obtained their numerical solution of Carreau fluid flow.

The current problem is an extension work to Raju and Sandeep [45]. The base paper is about unsteady Casson Carreau fluid, whereas the current analysis is steady Casson and Carreau nanofluid with slips and convective conditions. This work is not done by any other author. So it is a novel problem. The current work studies the computational analysis of three dimensional Casson and Carreau nanofluid flow due to a permeable stretching surface concerning the convective conditions. After using appropriate self-similarity functions the flow equations are modified to a system of nonlinear ODEs. The solution to the modified system is evaluated by numerical technique. The significant results are to inquire the impacts of involving variables on flow characteristics. We have evaluated the outcomes to the friction factors. The outcomes to local Nusselt are evaluated. The Sherwood number are evaluated. Favorable comparison is performed with before available outcomes for correlating the present results. The achieved results are in agreement with the ones of other scientific studies. The solution is presented for flow characteristics in the case of Casson and Carreau fluids.

2. Equations of Motion

Take three dimensional flows of Casson and Carreau nanofluids through a stretching sheet under convective conditions. Non-linear thermal radiation is incorporated. The non-uniform heat source/sink is included. The flow is confined with z-axis. The rheological version to an isotropic flow for Casson fluid is defined by [42, 43]:

$$\frac{1}{\tau^{-\frac{1}{n}}}=\frac{1}{\tau_0^{-\frac{1}{n}}}+\frac{1}{\mu\dot{\gamma}^{-\frac{1}{n}}} \tag{1}$$

$$\tau_{ij}=\begin{cases}2\left(\mu_B+p_z\left(2\pi\right)^{-0.5}\right)e_{ij},\ \pi>\pi_C\\ 2\left(\mu_B+p_z\left(2\pi\right)^{-0.5}\right)e_{ij},\ \pi<\pi_C\end{cases} \tag{2}$$

Critical value of π based on the non-Newtonian replica, the plastic dynamic viscosity of non-Newtonian fluid, and yield stress of the fluid are denoted by π_c , μ_B , p_z respectively. Here $\pi=e_{ij}e_{ij}$ and deformation rate's (i, j) the component is e_{ij} . π is the product of part of deformation rate with itself. The investigators have proposed the estimate for n as 1. But this estimate is more than 1 in several practices. The linear stretching produces flow. The Carreau fluid's extra stress tensor is defined as [44, 45]

$$\bar{\tau}_{ij} = \eta_0 \left[1 + 0.5 \left(\frac{1}{n-1} \right)^{-1} \left(\Gamma \bar{\dot{\gamma}} \right)^2 \bar{\dot{\gamma}}_{ij} \right] \tag{3}$$

Here the extra stress tensor, zero shear rate viscosity, time constant and power-law index are denoted by $\bar{\tau}_{ij}$, η_0, Γ, n and $\bar{\dot{\gamma}}$ is given by

$$\bar{\dot{\gamma}} = \sqrt{\frac{1}{2} \sum_i \sum_j \bar{\dot{\gamma}}_{ij} \bar{\dot{\gamma}}_{ji}} = \sqrt{\frac{1}{2}}\, \Pi \tag{4}$$

Here the second invariant strain Tensor is Π. The flow equations are defined as

$$\left(\frac{\partial x}{\partial u} \right)^{-1} + \left(\frac{\partial y}{\partial v} \right)^{-1} + \left(\frac{\partial z}{\partial w} \right)^{-1} = 0 \tag{5}$$

$$\left(u \left(\frac{\partial x}{\partial u} \right)^{-1} + v \left(\frac{\partial y}{\partial v} \right)^{-1} + w \left(\frac{\partial z}{\partial w} \right)^{-1} \right) = \nu \left((1 + \beta^{-1}) \frac{\partial^2 u}{\partial z^2} + 1.5(n-1)\Gamma^2 \left(\frac{\partial u}{\partial z} \right)^2 \frac{\partial^2 u}{\partial z^2} \right) - \sigma B_0^2 u \rho^{-1} - \nu k_p^{-1} u \tag{6}$$

$$u \left(\frac{\partial x}{\partial u} \right)^{-1} + v \left(\frac{\partial y}{\partial v} \right)^{-1} + w \left(\frac{\partial z}{\partial v} \right)^{-1} = \nu \left((1 + \beta^{-1}) \frac{\partial^2 v}{\partial z^2} + 1.5(n-1)\Gamma^2 \left(\frac{\partial v}{\partial z} \right)^2 \frac{\partial^2 v}{\partial z^2} \right) - \sigma B_0^2 v \rho^{-1} - \nu k_p^{-1} v \tag{7}$$

$$u \left(\frac{\partial x}{\partial u} \right)^{-1} + v \left(\frac{\partial y}{\partial T} \right)^{-1} + w \left(\frac{\partial z}{\partial T} \right)^{-1} = \alpha_1 \left(\frac{\partial z^2}{\partial^2 T} \right)^{-1} + q''' + \mu(1 + \beta^{-1}) \left(\frac{\partial u}{\partial y} \right)^2 + \tau \left[D_B \frac{\partial C}{\partial z} \frac{\partial T}{\partial z} + D_T T_\infty^{-1} \left(\frac{\partial T}{\partial y} \right)^2 \right] \tag{8}$$

$$u \left(\frac{\partial x}{\partial a_1} \right)^{-1} + v \left(\frac{\partial y}{\partial a_1} \right)^{-1} + w \left(\frac{\partial z}{\partial a_1} \right)^{-1} = D_{A_1} \left(\frac{\partial z^2}{\partial^2 a_1} \right)^{-1} - k_c a_1 b_1^2, \tag{9}$$

$$u \left(\frac{\partial x}{\partial b_1} \right)^{-1} + v \left(\frac{\partial y}{\partial b_1} \right)^{-1} + w \left(\frac{\partial z}{\partial b_1} \right)^{-1} = D_{B_1} \left(\frac{\partial z^2}{\partial^2 a_1} \right)^{-1} + k_c a_1 b_1^2, \tag{10}$$

The parts of velocity alongside the x, y and z axes are u, v and w respectively. The kinematic viscosity, magnetic induction, Casson fluid parameter, time constant, density of the fluid and electric conductivity are ν, B_0, β, Γ, ρ, σ respectively accompanying the boundary restrictions

$$\begin{aligned} &\frac{u - u_w(x)}{k} = \left(\frac{\partial y}{\partial u} \right)^{-1} = ax, \quad v = v_w(x) = ax, \\ &w = 0, \quad \frac{-k}{h_f} \left(\frac{\partial z}{\partial T} \right)^{-1} = \left(T_f - T \right), \\ &\left(\frac{\partial z}{\partial a_1} \right)^{-1} = \frac{k_s a_1}{D_{A_1}}, \left(\frac{\partial z}{\partial b_1} \right)^{-1} = \frac{-k_s a_1}{D_{B_1}}, \\ &u = v = 0, \ T \to T_\infty, \ a_1 \to a_0, \ b_1 \to 0, \ \text{as } z \to \infty \end{aligned} \tag{11}$$

The stretching velocities close to the surface are u_w and v_w. We define the following relation as

$$\begin{aligned} &T - T_\infty = (T_w - T_\infty)\theta \\ &\frac{T}{T_\infty} = \left(1 + (\theta_w - 1)\theta \right) \end{aligned} \tag{12}$$

The non-uniform heat source/sink q''' which is time dependent is given as:

$$q''' = \frac{k_f u_w(x)}{x\nu} \left(A(T_w - T_\infty) f_\eta + B(T - T_\infty) \right) \tag{13}$$

The positive estimates of A, B in equation (13) correspond to heat generation and negative estimations show heat absorption. For modification of the equations of motion (partial differential equations) to ODEs, utilize the following similarity functions:

$$f_\eta = \frac{u}{ax},\ g_\eta = \frac{v}{by},\quad f(\eta)+g(\eta) = -w\left(bv_f\right)^{-0.5},\ \eta = z\,b^{0.5}v_f^{-0.5} \tag{14}$$

The equation of continuity is fulfilled with u, v and w, and by substituting the Equations (14), in (6)-(10) we obtain

$$\left(1+\beta^{-1}+1.5(n-1)Wef_{\eta\eta}^2\right)f_{\eta\eta\eta}+(f+g)f_{\eta\eta}-f_\eta^2-\frac{1}{M^{-1}}f_\eta-\frac{1}{K_1^{-1}}f_\eta=0 \tag{15}$$

$$\left(1+\beta^{-1}+1.5(n-1)Weg_{\eta\eta}^2\right)g_{\eta\eta\eta}+(f+g)g_{\eta\eta}-{g_\eta}^2-\frac{1}{M^{-1}}g_\eta-\frac{1}{K_1^{-1}}g_\eta\ =0 \tag{16}$$

$$\begin{gathered}\theta_{\eta\eta}+\Pr\left[(f+g)\theta_\eta+Nt\,\theta_\eta^2+Nb\,\theta_\eta\varphi_\eta+E_c\left(1+\beta^{-1}\right)f_{\eta\eta}^2\right]+R\left[\left(1+(\theta_w-1)\theta\right)^3\theta_{\eta\eta}\right.\\ \left.+3(\theta_w-1)f_{\eta\eta}\theta_\eta^2\left(1+(\theta_w-1)\theta\right)^2+Af_\eta+B\theta=0\right.\end{gathered} \tag{17}$$

$$\left(Sc\right)^{-1}\varphi_{\eta\eta}+(f+g)\varphi_\eta-K\varphi(1-\varphi)^2=0 \tag{18}$$

$$\delta\left(Sc\right)^{-1}H_{\eta\eta}+(f+g)H_\eta+K\varphi H^2=0 \tag{19}$$

The dimensionless quantities are defined by

$$\varphi(\eta)=\frac{a_1}{a_0},\ H(\eta)=\frac{b_1}{a_0} \tag{20}$$

The altered boundary restrictions are given by

$$\begin{gathered}f(\eta)=0,\ g(\eta)=0,\ \frac{f_\eta-\lambda}{\alpha}=f_{\eta\eta},\ \frac{g_\eta-\lambda}{\alpha}=g_{\eta\eta}\\ -Bi_1=\frac{\theta_\eta}{1-\theta(\eta)},\ \varphi(\eta)=\varphi_\eta K_s^{-1},\ \delta K_s^{-1}H_\eta=-\varphi(\eta)\ \text{at}\ \eta=0\\ f_\eta,g_\eta,\theta(\eta),H(\eta)\to 0,\ \varphi(\eta)\to 1\ \text{ as }\ \eta\to\infty\end{gathered} \tag{21}$$

The Weissenberg number, magnetic field parameter, stretching ratio parameter, Prandtl number, thermal radiation parameter, ratio of temperatures, Schmidt number, strength of the chemical reactions parameter, ratio of diffusion coefficient of species A_1, diffusion coefficient of the species B_1, positive constant, concentrations of the chemical species and stretching ratio parameter are denoted by We, M, λ, Pr, R, θ_w, Sc, K_s, δ, D_{A_1}, D_{B_1}, a_0, a_1, b_1, k respectively. The physical variables are defined by

$$\begin{gathered}M=\sigma B_0\left(\rho_f a\right)^{-1},\ We=\Gamma^2x^2b^3v^{-1},\ \Pr=k\left(\mu C_p\right)^{-1},\ R=16\sigma^*T_\infty^3\left(3kk^*\right)^{-1},\ \theta_w=T_\infty T_w^{-1}\\ Sc=v_S D_{A_1}^{-1},\ \delta=D_{B_1}D_{A_1}^{-1},\ K=k_C a_0^2 b^{-1},\ K\,Sc\,D_{A_1}=K_S\left(v\right)^{1/2}\end{gathered}$$

For majority of practical utilizations the chemical diffusion coefficients are supposed to be almost identical. Diffusion coefficients are identical. Therefore δ = 1. Then we obtain $\varphi(\eta)=1-H(\eta)$. The engineering quantities are the friction factor coefficients alongside x, y axes, local Nusselt and Sherwood numbers are defined as

$$\begin{gathered}C_{fx}=\mathrm{Re}^{-1/2}\left(\left(1+\beta^{-1}\right)f_{\eta\eta}+0.5\left(\frac{1}{(n-1)We}\right)^{-1}(f_{\eta\eta})^3\right)\\ C_{fy}=\mathrm{Re}^{-1/2}\left(\left(1+\beta^{-1}\right)g_{\eta\eta}+0.5\left(\frac{1}{(n-1)We}\right)^{-1}(g_{\eta\eta})^3\right)\\ Nu_x=-\mathrm{Re}^{1/2}\,\theta_\eta(0),\ Sh_x=-\mathrm{Re}^{1/2}\,\varphi_\eta(0)\end{gathered} \tag{22}$$

Here the Reynolds number is defined by $\mathrm{Re}=x\,u_w(x)v^{-1}$.

3. Results and Discussion

The solutions to converted equations of motion (9) together with boundary conditions (10) are evaluated via Runge-Kutta fourth order procedure alongside shooting mechanism. The obtained results are inspected with previous solutions obtained by Raju et al. [17]. They are matched with them for special cases. The comparative study of present results with those obtained by Raju et al. [17] and Raju and Sandeep [45] is shown in Tables 2 and 3. Analysis of the present estimates is made by keeping the following values for the involved variables: Pr = 6.2, $Nt = Nb = 0.6$, $E_c = \alpha = \beta = 0.2$, $\lambda = A = Bi_1 = K = 0.1$, $K = K_S = 1$, $B = We = 0.3$, $M = 2$, $n = 3$, $Sc = 0.6$. Tables 1 & 2 are formulated for showing the validation of evaluated outcomes by giving comparison to Raju et al. [17] and Raju and Sandeep [45]. By observing these tables we came to a conclusion that skin friction factors are improved for larger *M*. But the negative trend is seen for the local Nusselt number as well as Sherwood number through *M*. These tables show that the results are in good agreement of evaluated outputs with those obtained by Raju and Sandeep [45].

Table 1. Comparative estimate of skin friction factors with the previously published values when the values of parameters $We, \eta, n, A, B, R, \theta_w, K, K_S, \Pr, Sc$ are taken zero.

β	M	$\lambda = 0$			$\lambda = 0.5$		
		Raju and Sandeep [45] C_{fx}	Present Estimates C_{fx}	Raju and Sandeep [45] C_{fx}	Raju and Sandeep [45] C_{fy}	Present Estimates C_{fy}	Raju and Sandeep [45] C_{fy}
1		1.4142	1.4142	1.5459	0.6579	1.5459	0.6579
5	0	1.0954	1.0952	1.1974	0.5096	1.1980	0.5096
∞		1.0049	1.0049	1.0932	0.4653	1.0932	0.4653
1		4.6904	4.6904	4.7263	2.3276	4.7263	2.3276
5	10	3.6331	3.6331	3.6610	1.8030	3.6610	1.8030
∞		3.3165	3.3165	3.3420	1.6459	3.3420	1.6459
1		14.2127	14.212	14.2244	7.1004	14.224	7.1004
5	100	11.0091	11.009	11.0182	5.5000	11.017	5.4998
∞		10.0490	10.049	10.058	5.0208	10.058	5.0207

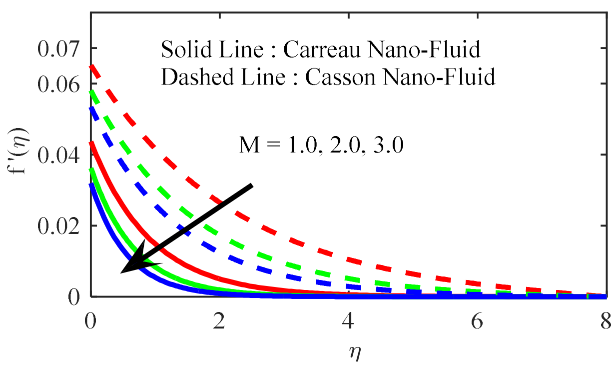

Fig. 1. $f'(\eta)$ via magnetic parameter

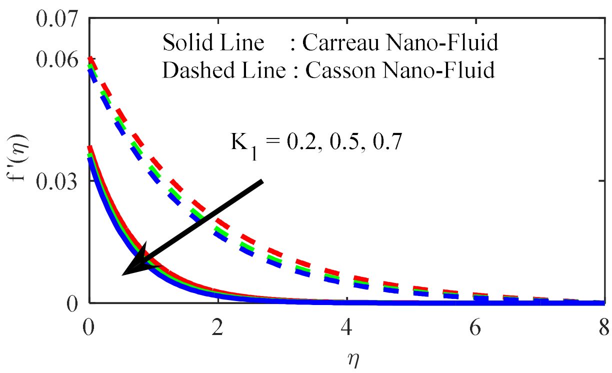

Fig. 2. $f'(\eta)$ via permeability parameter

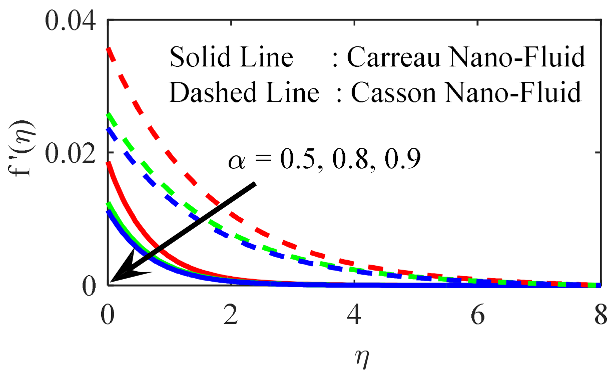

Fig. 3. $f'(\eta)$ via velocity slip parameter

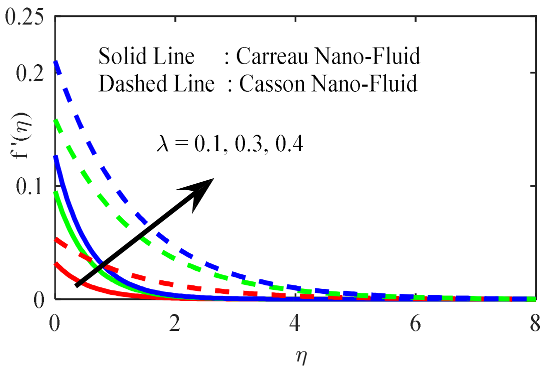

Fig. 4. $f'(\eta)$ via stretching ratio parameter

In this frame work, all the plots are drawn to show the variations in velocity profiles, energy as well as mass diffusion with different involved variables in regard of Casson and Carreau nanofluids. Investigation of velocity profile $f'(\eta)$ with different estimates of involved variables is sketched in Figs. 1-4. The plots from 1 to 3 show a descending tendency in velocity profiles with ascending values of magnetic, permeability and velocity slip parameters. The fact that velocity distribution of Casson nanofluid is dominant when compared to the velocity distribution of Carreau nanofluid, can be predicted from Figures 1 to 3. The drag force is generated by magnetic field for improvement in the estimates of M and depresses the velocity fields. The thickness of boundary layer is reduced for boosting estimates of magnetic parameter. This indicates that improvement in magnetic parameter causes to thin boundary layer. The velocity profile is highlighted with ascending estimates of stretching ratio parameter.

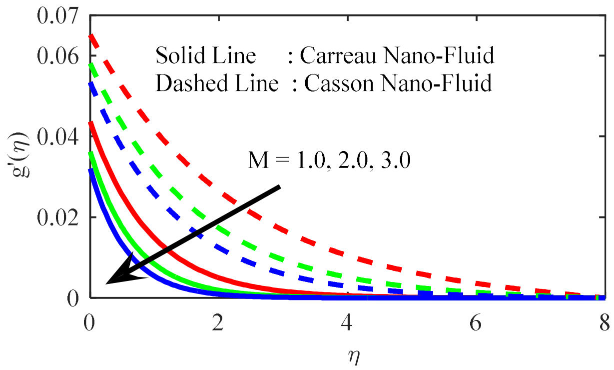

Fig. 5. $g'(\eta)$ via magnetic parameter

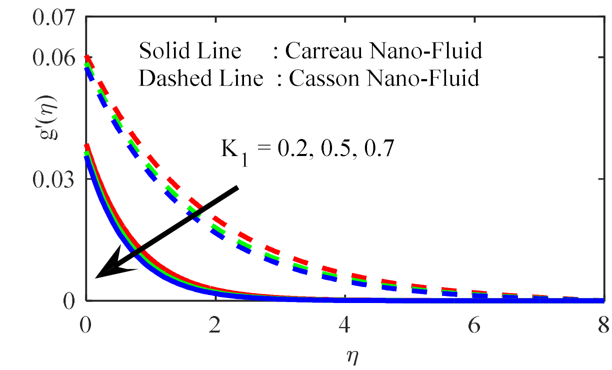

Fig. 6. $g'(\eta)$ via permeability parameter

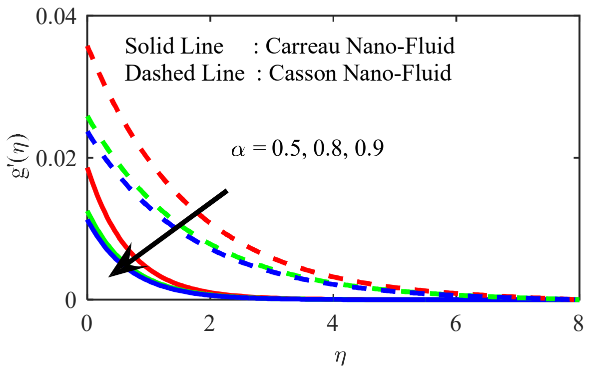

Fig. 7. $g'(\eta)$ via velocity slip parameter

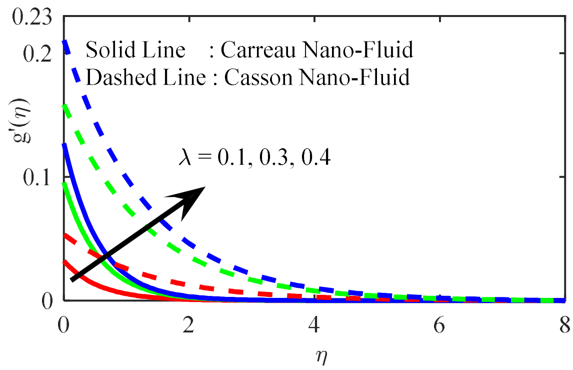

Fig. 8. $g'(\eta)$ via stretching ratio parameter

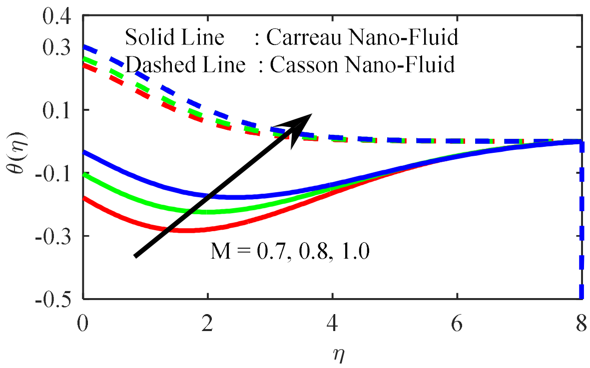

Fig. 9. $\theta(\eta)$ via magnetic parameter

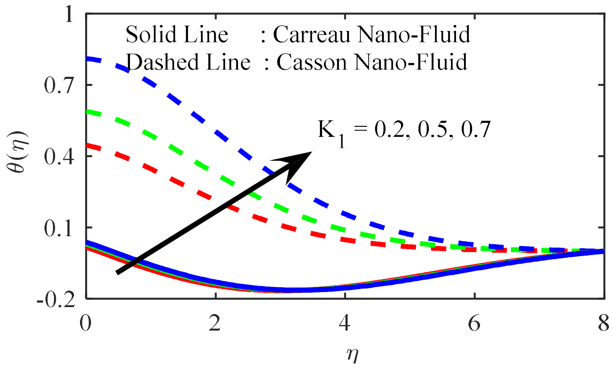

Fig. 10. $\theta(\eta)$ via permeability parameter

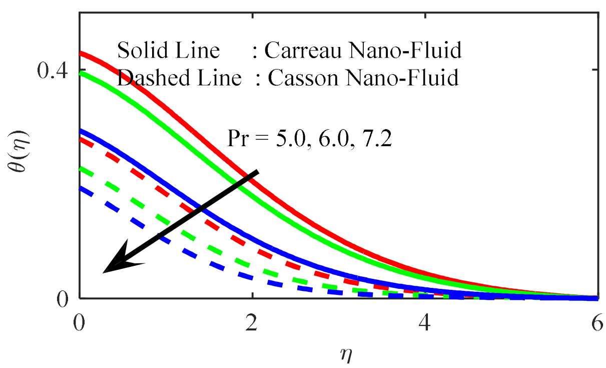

Fig. 11. $\theta(\eta)$ via Prandtl number

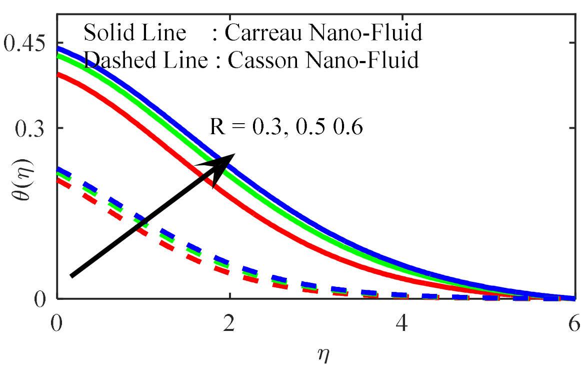

Fig. 12. $\theta(\eta)$ via radiation parameter

Table 2. Comparative estimates of Nusselt number with the previously published values when the estimates for the parameters $We, \eta, n, A, B, R, \theta_w, K, K_S, \Pr, Sc$ and $\beta \to \infty$ are taken zero.

λ	$\Pr = 0.7$			$\Pr = 1$		
	Raju et al. [17]	Raju and Sandeep [45]	Present output	Raju et al. [17]	Raju and Sandeep [45]	Present output
0	0.4769	0.4305	0.4307	0.5180	0.5572	0.5563
1	0.6004	0.6004	0.6003	0.7005	0.7219	0.7218
10	1.0097	1.0172	1.0175	1.1494	1.1709	1.1707

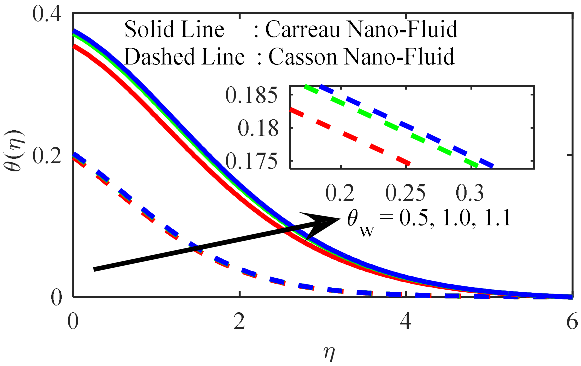

Fig. 13. $\theta(\eta)$ via temperature ratio parameter

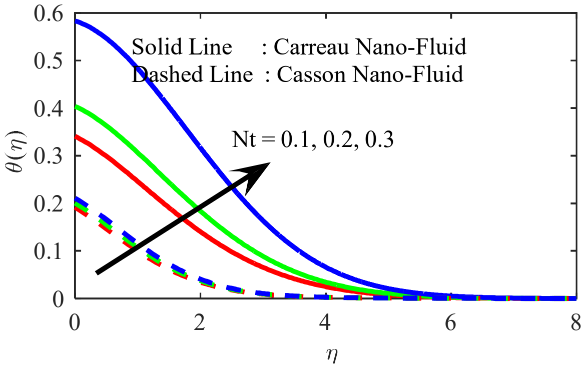

Fig. 14. $\theta(\eta)$ via thermophoresis parameter

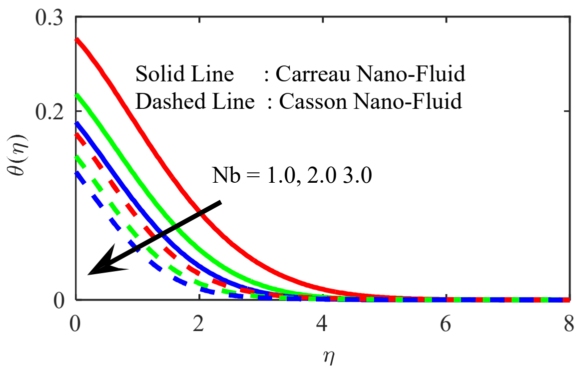

Fig. 15. $\theta(\eta)$ via Brownian motion parameter

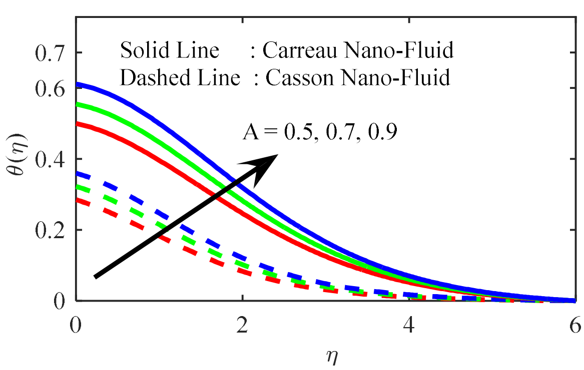

Fig. 16. $\theta(\eta)$ via non-uniform heat source/sink parameter

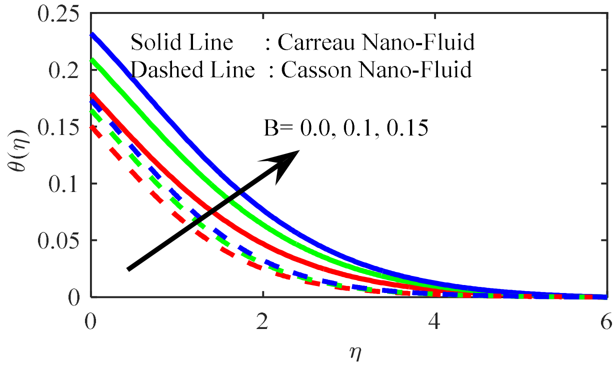

Fig. 17. $\theta(\eta)$ via non-uniform heat source/sink parameter

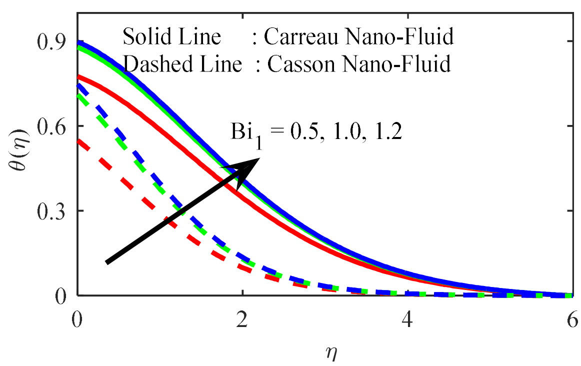

Fig. 18. $\theta(\eta)$ via thermal Biot number

This feature is predicted in Fig. 4. Figures 5 to 8 are plotted for showing the variations in velocity profiles $g'(\eta)$ with growing values of magnetic parameter, permeability parameter, velocity slip parameter and stretching ratio parameter. The results portrayed in Figs. 5 to 8 are exactly same for $g'(\eta)$ as that of $f'(\eta)$. These results are represented in Figs. 5 to 8. Figs. 9 to 10 are plots portraying the growing feature of temperature distribution in regard of important variables i.e. magnification in temperature distribution is appeared with enhanced values of magnetic, and permeability parameters. Carreau nano fluid has less energy distribution via magnetic and permeability parameter, than that of Casson nanofluid. The boosting estimates of Prandtl number improve the temperature distribution. This tendency is supplied in Fig. 11. The Prandtl number alters from one fluid to another fluid. Prandtl number's estimate is large when thermal conductivity is small and viscosity is large. Prandtl number's boosting estimate leads to less thermal diffusivity. The thickness of thermal boundary layer reduces via Prandtl number. Figures 12 and 14 are plots portraying the growing feature of temperature distribution in regard of important variables i.e. magnification in temperature distribution is appeared with enhanced values radiation parameter, temperature ratio parameter, and thermophores parameter. Fig. 15 is a plot showing the descending feature in temperature profile with rising estimates of Brownian motion parameter. The growing feature of temperature distribution in regard of important variables i.e. heat source parameters, thermal Biot number is portrayed in Figs. 16 to 18.

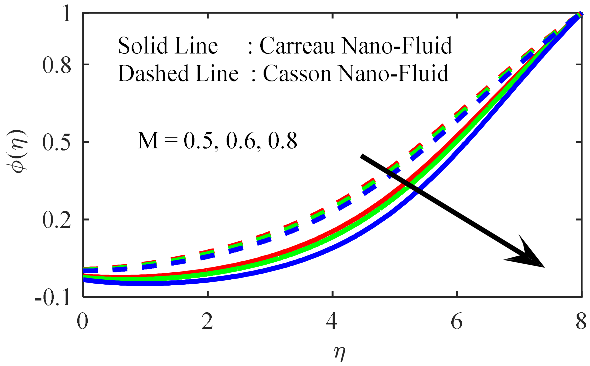

Fig. 19. $\phi(\eta)$ via magnetic parameter

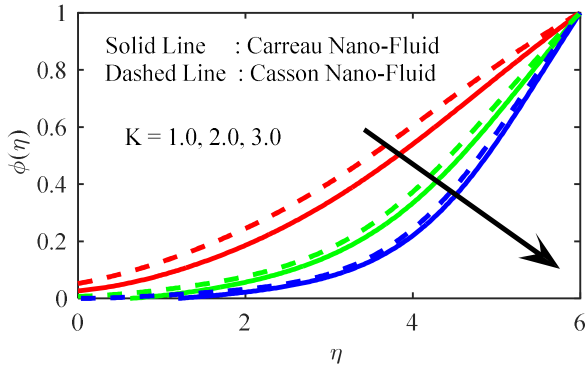

Fig. 20. $\phi(\eta)$ via strength of homogeneous reaction parameter

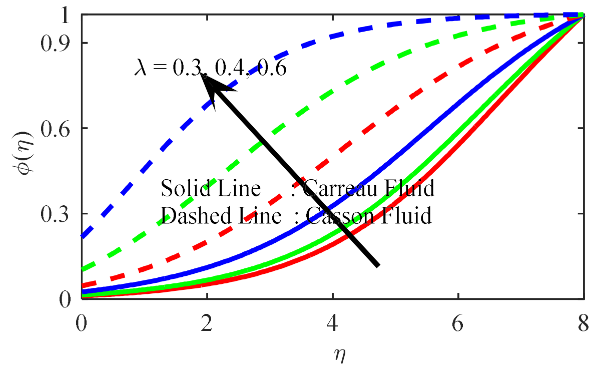

Fig. 21. $\phi(\eta)$ via stretching ratio parameter

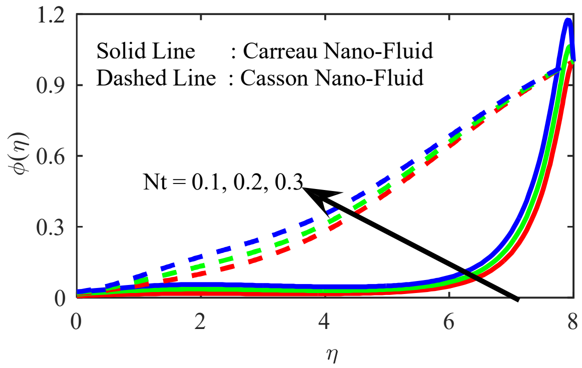

Fig. 22. $\phi(\eta)$ via thermophoresis parameter

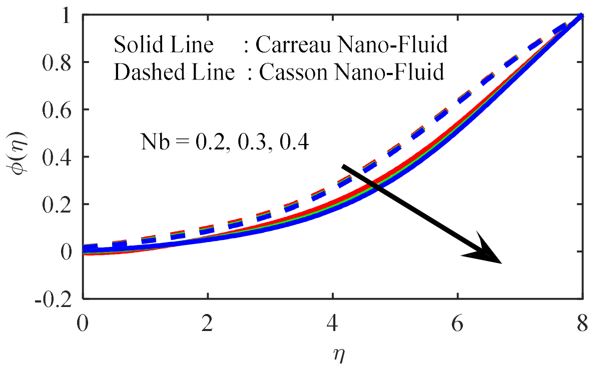

Fig. 23. $\phi(\eta)$ via Brownian motion parameter

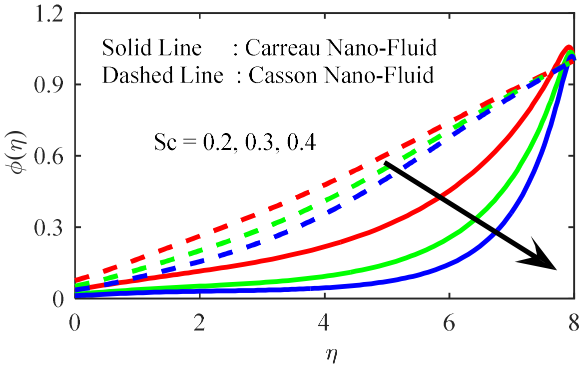

Fig. 24. $\phi(\eta)$ via Schmidt number

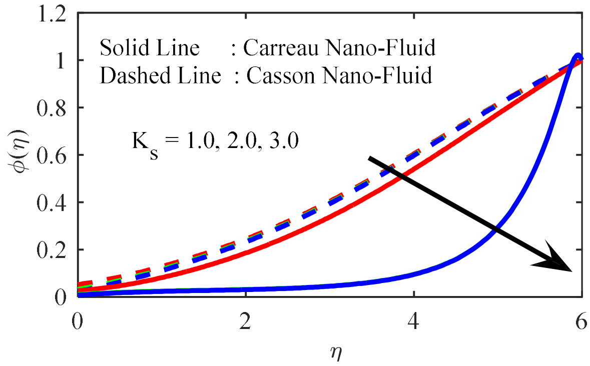

Fig. 25. $\phi(\eta)$ via strength of heterogeneous reaction parameter

Carreau nano fluid has more energy distribution via Prandtl number, thermal radiation parameter, the temperature ratio parameter, thermophoresis parameter, Brownian motion parameter, heat source/sink parameters, and thermal Biot number. Prediction of the effect of involved variables on concentration function is sketched in Figs. 19-25. The magnetic parameter and strength of the homogeneous reaction parameter decay the concentration distribution. Conversely, with greater estimations of stretching ratio parameter, and thermophoresis parameter on concentration distribution portrays the opposite outline. Conversely, with greater estimations of Brownian motion parameter, Schmidt number and strength of the heterogeneous reaction parameter upon concentration distribution portrays opposite outline. Improved estimates of Schmidt number show powerful molecular motions that magnify the temperature of the fluid. Carreau nanofluid has less concentration distribution via magnetic parameter and strength of the homogeneous reaction parameter, stretching ratio parameter, and thermophoresis parameter, thermophoresis parameter, Brownian motion parameter, Schmidt number and strength of the heterogeneous reaction parameter than that of Casson nanofluid.

4. Conclusion

The current work studied the computational analysis of three dimensional Casson and Carreau nanofluid flow concerning the convective conditions. After using appropriate self-similarity functions, the flow equations were modified to a system of nonlinear ODEs. The solution of the modified system was evaluated by numerical technique. The results showed the impacts of involving variables on flow characteristics. We also evaluated the outcomes to the friction factors. The outcomes to local Nusselt were evaluated. The outputs to Sherwood number were evaluated. Favorable comparison was performed with before available outcomes for correlating the present results. The achieved results were matched with solutions obtained by other researchers. The solution was presented for flow characteristics in the case of Casson and Carreau fluids. The following are some of the key observations:

- Velocities reduce for growing values of permeability and velocity slip parameters in the case of Casson and Carreau nanofluids.
- Temperature field enhances with the hike in the estimations of thermohoresis parameter and the thermal Biot number in case of Casson and Carreau nanofluids.
- Thermophoresis parameter's growing estimations magnify the concentration field, but for larger values of Brownian motion parameter reduce the temperature as well as concentration profile in case of Casson and Carreau nanofluids.
- Enhancing values of velocity slip parameter results in decrease in the skin friction coefficients, rate of heat transfer and increase in the rate of mass transfer in case of Casson and Carreau nanofluids.
- The hike in the thermal Biot number elevates temperature but reduces the rate of mass transfer in case of Casson and Carreau nanofluids.

Conflict of Interest

The authors declared no potential conflicts of interest with respect to the research, authorship and publication of this article.

Funding

The authors received no financial support for the research, authorship and publication of this article.

Nomenclature

A, B	Non uniform heat generation/absorption coefficients	Sc	Schmidt number
a, b	Rate constants	Sh_x	Local Sherwood number
a_0	Positive constants	T	Temperature of the fluid (K)
a_1, b_1	Concentration of chemical species	u, v, w	Velocity components in X, Y and Z directions respectively (m/s)
Bi_1	Thermal Biot number	We	Weissenberg number
B_0	Magnetic induction parameter	x	Distance along the surface (m)
C	Concentration of the fluid (Kg/m3)	y	Distance normal to the surface (m)
Cf_x	Skin friction Coefficient in x-direction	*Greek Symbols*	
Cf_y	Skin friction Coefficient in y -direction	α_1	Thermal diffusivity
c_P	Specific heat capacity at constant pressure (J/Kg K)	α	Velocity slip parameter
D_{A_1}, D_{B_1}	Diffusion coefficients	β	Casson fluid parameter
E_C	Eckert number	β_C	Concentration expansion coefficient
f, g	Dimensionless velocities	β_t	Volumetric thermal expansion
g	Acceleration due to gravity (m/s2)	δ	Ratio of diffusion coefficients

k	Thermal conductivity (W/m K)	η	Similarity variable
K_1	Permeability parameter	η_0	Zero shear rate viscosity
k^*	Mean absorption coefficient (m-1)	λ	Stretching ratio parameter
k_c, k_s	Rate constants	ϕ	Boundary layer concentration
K_s	Strength of heterogeneous reaction parameter	σ	Electrical conductivity
K	Strength of homogeneous reaction parameter	σ^*	Stefan Boltzmann coefficient
M	Magnetic field parameter	θ	Boundary layer temperature
n	Power-law index parameter	θ_W	Temperature ratio parameter
Nb	Brownian motion parameter	μ	Kinematic viscosity
Nt	Thermophoresis parameter	ν	Dynamic viscosity
Nu_x	Local Nusselt number	ρ	Density
P	Pressure (Pa or N/m)	*Subscripts*	
Pr	Prandtl number	f	Fluid
q'''	Non uniform heat source/sink (k/s)	w	Condition at the wall
R	Radiation parameter	∞	Condition at the free stream
Re	Local Reynolds number		

References

[1] Sakiadis, B.C., Boundary layer behaviour on continuous solid surfaces, *AICHE Journal*, 7(1), 1961, 26–28.

[2] Chamka, A.J., Aly, A.M., MHD free convection flow of a nanofluid past a vertical plate in the presence of heat generation or absorption effects, *Chemical Engineering Communications,* 198(3), 2010, 425–441.

[3] Hayat, T., Khan, M., Khan, M.I., Alsaedi, A., Ayub, M., Electromagnetic squeezing rotational flow of Carbon (C)-Water (H_2O) Kerosene oil nanofluid past a Riga plate: A numerical study, *PLOS ONE,* 12(8), 2017, 180976.

[4] Hsiao, K.L., To promote radiation electrical MHD activation energy thermal extrusion manufacturing system efficiency by using Carreau-Nanofluid with parameters control method, *Energy*, 130, 2017, 486-499.

[5] Nadeem, S., Haq, R.U.I., Akbar, N.S., Khan, Z.H., MHD three dimensional Casson fluid flow past a porous linearly stretching sheet, *Alexandria Engineering Journal*, 52, 2013, 577–582.

[6] Shehzad, S.A. , Hayat, T., Alsaedi, A., Three-dimensional MHD flow of Casson fluid in porous medium with heat generation, *Journal of Applied Fluid Mechanics*, 9, 2016, 215–223.

[7] Raju, C.S.K., Sandeep, N., Jayachandrababu, M., Sugunamma, V., Dual solutions for three-dimensional MHD flow of a nanofluid over a nonlinearly permeable stretching sheet, *Alexandria Engineering Journal*, 55(1), 2016, 151–162.

[8] Akbar, N.S., Nadeem, S., Khan, Z.H., Numerical simulation of peristaltic flow of a Carreau nanofluid in an asymmetric channel, *Alexandria Engineering Journal,* 53, 2014, 191–197.

[9] Akbar, N.S., Nadeem, S., Haq, R.U.I., Ye, S., MHD stagnation point flow of Carreau fluid toward a permeable shrinking sheet: dual solutions, *Ain Shams Engineering Journal*, 5, 2014, 1233–1239.

[10] Hayat, T., Bilal Ashraf, M., Shehzad, S.A., Alsaedi, A., Mixed convection flow of Casson nanofluid over a stretching sheet with convectively heated chemical reaction and heat source/sink, *Journal of Applied Fluid Mechanics*, 8, 2015, 803–813.

[11] Nagasantoshi, P., Ramana Reddy, G.V., Gnaneswara Reddy, M., Padma, P., Influence of Non-Uniform heat source on Casson and Carreau fluid flows over a stretching sheet with slip and convective conditions, *International Journal of Pure and Applied Mathematics,* 117(13), 2017, 363-371.

[12] Hsiao, K.L., Stagnation electrical MHD nanofluid mixed convection with slip boundary on a stretching sheet, *Applied Thermal Engineering,* 98, 2016, 850-861.

[13] Olanrewaju, P.O., Olanrewaju, M.A., Adesanya, A.O., Boundary layer flow of nanofluids over a moving surface in a flowing fluid in the presence of radiation, *International Journal of Applied Science and Technology*, 2(1), 2012, 274-285.

[14] Hsiao, K.L., Combined Electrical MHD Heat Transfer Thermal Extrusion System Using Maxwell Fluid with Radiative and Viscous Dissipation Effects, *Applied Thermal Engineering*, 112, 2016, 1281-1288.

[15] Hsiao, K.L., Micropolar nanofluid flow with MHD and viscous dissipation effects towards a stretching sheet with multimedia feature, *International Journal of Heat and Mass Transfer*, 112, 2017, 983-990.

[16] Sandeep, N., Sugunamma, V., Mohan Krishna, P., Effects of radiation on an unsteady natural convection flow of an E G Nimonic 80a nanofluid past an infinite vertical plate, *Journal of Theoretical and Applied Physics*, 23, 2013, 36–43.

[17] Raju, C.S.K., Jayachandrababu, M., Sandeep, N., Chemically reacting radiative MHD Jefferey nanofluid flow over a cone in porous medium, *International Journal of Engineering Research in Africa*, 19, 2016, 75–90.

[18] Saleem, N., Hayat, T., Alsaedi, A., Effectsof induced magnetic field and slip condition on peristaltic transport with heat and mass transfer in a non-uniform channel, *International Journal of Physical Sciences*, 7(2), 2012, 191-204.

[19] Sandeep, N., Sulochana, C., Dual solutions for unsteady mixed convection flow of MHD micropolar fluid over a

stretching/ shrinking sheet with non-uniform heat source/sink, *Engineering Science and Technology, an International Journal*, 18, 2015, 738–745.

[20] Raju, C.S.K., Sandeep, N., Sulochana, C., Sugunamma, V., Effects of aligned magnetic field and radiation on the flow of ferro fluids over a flat plate with non-uniform heat source/sink, *International Journal of Science and Engineering*, 8(2), 2015, 151–158.

[21] As, A., Zhou, Z., Hassan, M., Bhatti, M.M., Computational study of magnetized blood flow in the presence of Gyrotactic microorganisms propelled through a permeable capillary in a stretching motion, *International Journal for Multiscale Computational Engineering*, 16, 2018, 303-320.

[22] Bhatti, M.M., Lu, D.Q., Head-on collision between two hydro elastic solitary waves in shallow water, *Qualitative Theory of Dynamical Systems*, 17, 2018, 103-122

[23] Bhatti, M.M., Lu, D.Q., Analytical Study of the Head-On Collision Process between Hydroelastic Solitary Waves in the Presence of a Uniform Current, *Symmetry*, 11, 2019, 333.

[24] Bhatti, M.M., Rashidi, M.M., Effects of thermo-diffusion and thermal radiation on Williamson nanofluid over a porous shrinking/stretching sheet, *Journal of Molecular Liquids*, 221, 2016, 567-573

[25] Nagasantoshi, P., Ramana Reddy, G.V., Gnaneswara Reddy, M., Padma, P., Heat and mass transfer of Non-Newtonian Nanofluid flow over a stretching sheet with non-uniform heat source and Variable viscosity, *Journal of Nanofluids,* 7, 2018, 821-832.

[26] Hayat, T., Khan, M.I., Farooq, M., Alsaedi, A., Waqas, M., Yasmeen, T., Impact of Cattaneo–Christov heat flux model in flow of variable thermal conductivity fluid over a variable thicked surface, *International Journal of Heat and Mass Transfer,* 99, 2016, 702–710.

[27] Hayat, T., Khan, M.I., Farooq, M., Yasmeen, T., Alsaedi, A., Stagnation point flow with Cattaneo-Christov heat flux and homogeneous-heterogeneous reactions, *Journal of Molecular Liquids,* 220, 2016, 49-55.

[28] Khan, M.I., Waqas, M., Hayat, T., Alsaedi, A., A comparative study of casson fluid with homogeneous-heterogeneous reactions, *Journal of Colloid and Interface Science,* 298(15), 2017, 85.

[29] Khan, M.I., Waqas, M., Hayat, T., Imran Khan, M., Alsaedi, A., Numerical simulation of nonlinear thermal radiation and homogeneous-heterogeneous reactions in convective flow by a variable thicked surface, *Journal of Molecular Liquids,* 246, 2017, 259-267.

[30] Annimasun, I.L., Raju, C.S.K., Sandeep, N., Unequal diffusivities case of homogeneous–heterogeneous reactions within viscoelastic fluid flow in the presence of induced magnetic-field and nonlinear thermal radiation, *Alexgrandia Engineering Journal,* 55(2), 2016, 1595–1606.

[31] Khan, M.I., Hayat, T., Imran Khan, M., Alsaedi, A., Activation energy impact in nonlinear radiative stagnation point flow of Cross nanofluid, *International Communications in Heat and Mass Transfer,* 91, 2018, 216-224.

[32] Bhatti, M.M., Abbas, T., Rashidi, M.M., Sayed Ali, M.E.I., Yang, Z., Entropy generation on MHD Eyring–Powell nanofluid through a permeable stretching surface, *Entropy*, 18, 2016, 224.

[33] Hayat, T., Khan, M.I., Quayyam, S., Alsaedi, A., Entropy generation in flow with silver and copper nanoparticles, Colloids and surfaces A, *Physicochemecal and Engineering Aspects,* 539, 2018, 335-346.

[34] Hayat, T., Quayyam, S., Khan, M.I., Alsaedi, A., Entropy generation in magnetohydrodynamic radiative flow due to rotating disk in presence of viscous dissipation and Joule heating, *Physics of Fluids*, 30, 2018, 017101.

[35] Waleed, M., Khan, A., Khan, M.I., Hayat, T., Entropy generation minimization (EGM) of nanofluid flow by a thin moving needle with nonlinear thermal radiation, *Physica B: Condensed Matters,* 534, 2018, 113-119.

[36] Hayat, T., Khan, M.I., Quayyam, S., Alsaedi, A., Imran Khan, M., New thermodynamics of entropy generate on minimization with nonlinear thermal radiation and nano materials, *Physics Letters A,* 532(11), 2018, 749-760.

[37] Khan, M.I., Ullah, S., Hayat, T., Imran Khan, M., Alsaedi, A., Entropy generation minimization (EGM) for convection nanomaterial flow with nonlinear radiative heat flux, *Journal of Molecular Liquids,* 260, 2018, 279-291.

[38] Khan, M.I., Qayyum, S., Hayat, T., Imran Khan, M., Alsaedi, A., Ahmad Khan, T., Entropy generation in radiative motion of tangent hyperbolic nanofluid in presence of activation energy and nonlinear mixed convection, *Physics Letters A,* 382(31), 2018, 2017-2026.

[39] Khan, N.B., Ibrahim, Z., Khan, M.I., Hayat, T., Javeed, M.F., VIV study of an elastically mounted cylinder having low mass-damping ratio using RANS model, *International Journal of Heat and Mass Transfer,* 121, 2018, 309-314.

[40] Hayat, T., Khan, M.I., Quayyam, S., Alsaedi, A., Modern developments about statistical declaration and probable error for skin friction and Nusselt number with copper and silver nanoparticles, *Chinese Journal of Physics,* 55(6), 2017, 2501-2513.

[41] Raju, C.S.K., Sandeep, N., Sugunamma, V., Jayachandrababu, M., Ramanareddy, J.V., Heat and mass transfer in magnetohydrodynamic Casson fluid over an exponentially permeable stretching surface, *Engineering Science and Technology, an International Journal,* 19, 2016, 45-52.

[42] Hayat, T., Shezad, S. A., Alsaedi, A., Soret and Dufour effects in magnetohydrodynamic (MHD) flow of Casson fluid, *Applied Mathematics and Mechanics*, 33, 2012, 1301-1312.

[43] Ali, M.E., Sandeep, N., Cattaneo-Christov model for radiative heat transfer of magnetohydrodynamic Casson-ferrofluid: a numerical study, *Results in Physics*, 7, 2017, 21–30.

[44] Hayat, T., Asad, S., Mustafa, M., Alsaedi, A., Boundary layer flow of Carreau fluid over a convectively heated stretching sheet, *Applied Mathematics and Computation,* 246, 2014, 12–22.

[45] Raju, C.S.K., Sandeep, N., Unsteady three-dimensional flow of Casson–Carreau fluids past a stretching surface,

Alexandria Engineering Journal, 55, 2016, 1115–1126.

ORCID iD

G.V. Ramana Reddy https://orcid.org/0000-0002-6455-3750

© 2020 by the authors. Licensee SCU, Ahvaz, Iran. This article is an open access article distributed under the terms and conditions of the Creative Commons Attribution-NonCommercial 4.0 International (CC BY-NC 4.0 license) (http://creativecommons.org/licenses/by-nc/4.0/).